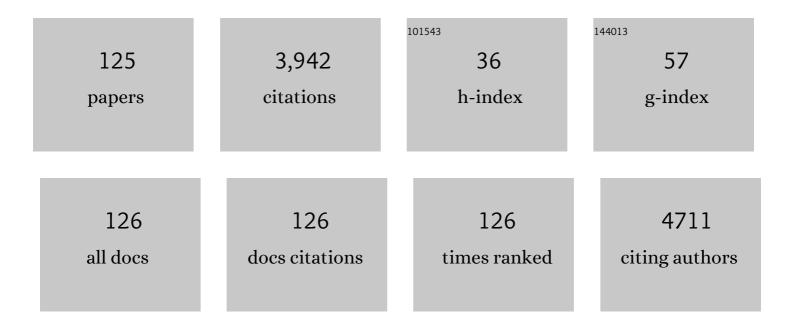
## Francois Lagugne-Labarthet

List of Publications by Year in descending order

Source: https://exaly.com/author-pdf/2338385/publications.pdf Version: 2024-02-01



#	Article	IF	CITATIONS
1	Optical Resonances of Chiral Metastructures in the Midâ€infrared Spectral Range. Israel Journal of Chemistry, 2023, 63, .	2.3	2
2	Investigating the Performances of Wide-Field Raman Microscopy with Stochastic Optical Reconstruction Post-Processing. Applied Spectroscopy, 2022, 76, 340-351.	2.2	7
3	Correction: Extending nanoscale patterning with multipolar surface plasmon resonances. Nanoscale, 2021, 13, 13905-13905.	5.6	0
4	Single-beam inscription of plasmon-induced surface gratings. Optical Materials, 2021, 112, 110775.	3.6	2
5	Ultrafiltration and Injection of Islet Regenerative Stimuli Secreted by Pancreatic Mesenchymal Stromal Cells. Stem Cells and Development, 2021, 30, 247-264.	2.1	7
6	Exploiting Light Interferences to Generate Micrometerâ€High Superstructures from Monomeric Azo Materials with Extensive Orientational Mobility. Advanced Optical Materials, 2021, 9, 2100525.	7.3	4
7	Characterization of extracellular vesicles derived from mesenchymal stromal cells by surface-enhanced Raman spectroscopy. Analytical and Bioanalytical Chemistry, 2021, 413, 5013-5024.	3.7	17
8	Three-color plasmon-mediated reduction of diazonium salts over metasurfaces. Nanoscale Advances, 2021, 3, 2501-2507.	4.6	2
9	Extending nanoscale patterning with multipolar surface plasmon resonances. Nanoscale, 2021, 13, 11051-11057.	5.6	4
10	Characterization of ovarian cancer-derived extracellular vesicles by surface-enhanced Raman spectroscopy. Analyst, The, 2021, 146, 7194-7206.	3.5	13
11	Investigation of Au SAMs Photoclick Derivatization by PM-IRRAS. Langmuir, 2020, 36, 1014-1022.	3.5	7
12	Second-Harmonic Generation from Dendritic Fractal Structures. Plasmonics, 2020, 15, 507-515.	3.4	5
13	Deciphering tip-enhanced Raman imaging of carbon nanotubes with deep learning neural networks. Physical Chemistry Chemical Physics, 2020, 22, 17857-17866.	2.8	4
14	Sierpiński Fractals as Plasmonic Metastructures for Second-Harmonic Generation. ACS Applied Nano Materials, 2020, 3, 3922-3929.	5.0	4
15	Hierarchical Plasmon Resonances in Fractal Structures. ACS Photonics, 2020, 7, 1246-1254.	6.6	12
16	GSK3787-Loaded Poly(Ester Amide) Particles for Intra-Articular Drug Delivery. Polymers, 2020, 12, 736.	4.5	5
17	Surface Plasmon Resonance Mode Behaviour in Sierpinski Fractal Triangles and New Plasmonic Materials. Microscopy and Microanalysis, 2019, 25, 636-637.	0.4	0
18	Fabrication and In Situ Cross-Linking of Carboxylic-Acid-Functionalized Poly(Ester Amide) Scaffolds for Tissue Engineering. ACS Applied Polymer Materials, 2019, 1, 2360-2369.	4.4	8

#	Article	IF	CITATIONS
19	In search of the hot spot. Nature Nanotechnology, 2019, 14, 922-923.	31.5	6
20	Carving Plasmon Modes in Silver Sierpiński Fractals. ACS Photonics, 2019, 6, 2974-2984.	6.6	9
21	Advancements in fractal plasmonics: structures, optical properties, and applications. Analyst, The, 2019, 144, 13-30.	3.5	40
22	Optoelectronic, Aggregation, and Redox Properties of Doubleâ€Rotor Boron Difluoride Hydrazone Dyes. Chemistry - A European Journal, 2019, 25, 5994-6006.	3.3	28
23	Trapping and SERS identification of extracellular vesicles using nanohole arrays. , 2019, , .		6
24	Probing mid-infrared plasmon resonances in extended radial fractal structures. Optics Letters, 2019, 44, 3865.	3.3	6
25	Exploiting Anisotropy of Plasmonic Nanostructures with Polarization Modulation Infrared Linear Dichroism Microscopy (ÂμΡMâ€IRLD). Advanced Optical Materials, 2018, 6, 1701336.	7.3	15
26	A Mass-Producible and Versatile Sensing System: Localized Surface Plasmon Resonance Excited by Individual Waveguide Modes. ACS Sensors, 2018, 3, 334-341.	7.8	6
27	Second harmonic generation microscopy from non-centrosymmetric gold half-coated polystyrene spheres. Surface Science, 2018, 676, 46-50.	1.9	0
28	Microencapsulation by <i>in situ</i> Polymerization of Amino Resins. Polymer Reviews, 2018, 58, 326-375.	10.9	55
29	Icephobic Behavior of UV-Cured Polymer Networks Incorporated into Slippery Lubricant-Infused Porous Surfaces: Improving SLIPS Durability. ACS Applied Materials & Interfaces, 2018, 10, 2890-2896.	8.0	97
30	Optical near-field mapping of plasmonic nanostructures prepared by nanosphere lithography. Beilstein Journal of Nanotechnology, 2018, 9, 1536-1543.	2.8	1
31	A π-conjugated inorganic polymer constructed from boron difluoride formazanates and platinum( <scp>ii</scp> ) diynes. Chemical Communications, 2018, 54, 6899-6902.	4.1	36
32	Imaging the Surface of a Hand-Colored 19th Century Daguerreotype. Applied Spectroscopy, 2018, 72, 1215-1224.	2.2	7
33	Plasmon-Mediated Drilling in Thin Metallic Nanostructures. ACS Omega, 2018, 3, 7269-7277.	3.5	7
34	Analytical Considerations in Nanoscale Flow Cytometry of Extracellular Vesicles to Achieve Data Linearity. Thrombosis and Haemostasis, 2018, 118, 1612-1624.	3.4	34
35	Luminescent CdSe Superstructures: A Nanocluster Superlattice and a Nanoporous Crystal. Journal of the American Chemical Society, 2017, 139, 1129-1144.	13.7	21
36	Dendritic Plasmonics for Mid-Infrared Spectroscopy. Journal of Physical Chemistry C, 2017, 121, 9497-9507.	3.1	33

#	Article	IF	CITATIONS
37	Tip-enhanced Raman spectroscopy of amyloid $\hat{I}^2$ at neuronal spines. Analyst, The, 2017, 142, 4415-4421.	3.5	31
38	Recent Advances of Plasmon-Enhanced Spectroscopy at Bio-Interfaces. ACS Symposium Series, 2016, , 183-207.	0.5	5
39	Tip-enhanced Raman spectroscopy: plasmid-free vs. plasmid-embedded DNA. Analyst, The, 2016, 141, 3251-3258.	3.5	27
40	A nanoaggregate-on-mirror platform for molecular and biomolecular detection by surface-enhanced Raman spectroscopy. Analytical and Bioanalytical Chemistry, 2016, 408, 609-618.	3.7	9
41	Photocontrolled Degradation of Stimuli-Responsive Poly(ethyl glyoxylate): Differentiating Features and Traceless Ambient Depolymerization. Macromolecules, 2016, 49, 7196-7203.	4.8	38
42	Superimposed Arrays of Nanoprisms for Multispectral Molecular Plasmonics. ACS Photonics, 2016, 3, 1723-1732.	6.6	30
43	Probing the Plasmonic Properties of Heterometallic Nanoprisms with Near-Field Fluorescence Microscopy. Journal of Physical Chemistry C, 2016, 120, 20267-20276.	3.1	14
44	Second harmonic generation from gold meta-molecules with three-fold symmetry. Physical Chemistry Chemical Physics, 2016, 18, 7956-7965.	2.8	19
45	The role of bone sialoprotein in the tendon–bone insertion. Matrix Biology, 2016, 52-54, 325-338.	3.6	17
46	Controlled positioning of analytes and cells on a plasmonic platform for glycan sensing using surface enhanced Raman spectroscopy. Chemical Science, 2016, 7, 575-582.	7.4	31
47	Tip-enhanced Raman spectroscopy of graphene-like and graphitic platelets on ultraflat gold nanoplates. Physical Chemistry Chemical Physics, 2015, 17, 21315-21322.	2.8	34
48	Photochromic Organic Nanoparticles as Innovative Platforms for Plasmonic Nanoassemblies. ACS Applied Materials & Interfaces, 2015, 7, 1932-1942.	8.0	24
49	Au Nanostructured Surfaces for Electrochemical and Localized Surface Plasmon Resonance-Based Monitoring of α-Synuclein–Small Molecule Interactions. ACS Applied Materials & Interfaces, 2015, 7, 4081-4088.	8.0	29
50	Enhanced Rates of Photoinduced Molecular Orientation in a Series of Molecular Glassy Thin Films. Langmuir, 2015, 31, 7296-7305.	3.5	7
51	Hydroxyapatite Growth Inhibition Effect of Pellicle Statherin Peptides. Journal of Dental Research, 2015, 94, 1106-1112.	5.2	34
52	Tunable 3D Plasmonic Cavity Nanosensors for Surface-Enhanced Raman Spectroscopy with Sub-femtomolar Limit of Detection. ACS Photonics, 2015, 2, 752-759.	6.6	80
53	Gold nanosponges (AuNS): a versatile nanostructure for surface-enhanced Raman spectroscopic detection of small molecules and biomolecules. Analyst, The, 2015, 140, 7278-7282.	3.5	7
54	High-resolution Raman imaging of bundles of single-walled carbon nanotubes by tip-enhanced Raman spectroscopy. Canadian Journal of Chemistry, 2015, 93, 51-59.	1.1	5

#	Article	IF	CITATIONS
55	Towards attomolar detection using a surface-enhanced Raman spectroscopy platform fabricated by nanosphere lithography. Canadian Journal of Chemistry, 2014, 92, 1-8.	1.1	15
56	Imaging the Optical near Field in Plasmonic Nanostructures. Applied Spectroscopy, 2014, 68, 1307-1326.	2.2	35
57	Plasmonic nanostructures for enhanced Raman spectroscopy: SERS and TERS of thiolated monolayers. Proceedings of SPIE, 2014, , .	0.8	3
58	On the absorption and electromagnetic field spectral shifts in plasmonic nanotriangle arrays. Optics Express, 2014, 22, 13308.	3.4	12
59	Nanoparticle Organization through Photoinduced Bulk Mass Transfer. Langmuir, 2014, 30, 2926-2935.	3.5	18
60	Microfluidic channel with embedded SERS 2D platform for the aptamer detection of ochratoxin A. Analytical and Bioanalytical Chemistry, 2013, 405, 1613-1621.	3.7	98
61	Tip-Enhanced Raman Spectroscopy of Self-Assembled Thiolated Monolayers on Flat Gold Nanoplates Using Gaussian-Transverse and Radially Polarized Excitations. Journal of Physical Chemistry C, 2013, 117, 15639-15646.	3.1	34
62	Optical Properties of Silver and Gold Tetrahedral Nanopyramid Arrays Prepared by Nanosphere Lithography. Journal of Physical Chemistry C, 2013, 117, 14778-14786.	3.1	92
63	Directing GPCR-transfected cells and neuronal projections with nano-scale resolution. Biomaterials, 2013, 34, 10065-10074.	11.4	8
64	Localized enhancement of electric field in tip-enhanced Raman spectroscopy using radially and linearly polarized light. Optics Express, 2013, 21, 25271.	3.4	75
65	Tip-Enhanced Raman Imaging and Nano Spectroscopy of Etched Silicon Nanowires. Sensors, 2013, 13, 12744-12759.	3.8	22
66	Tip-enhanced Raman spectroscopy: application to the study of single silicon nanowire and functionalized gold surface. Proceedings of SPIE, 2012, , .	0.8	1
67	Surface-Enhanced Fluorescence: Mapping Individual Hot Spots in Silica-Protected 2D Gold Nanotriangle Arrays. Journal of Physical Chemistry C, 2012, 116, 11665-11670.	3.1	39
68	Studies of the interaction of two organophosphonates with nanostructured silver surfaces. Analyst, The, 2012, 137, 4448.	3.5	28
69	Label-Free Mapping of Osteopontin Adsorption to Calcium Oxalate Monohydrate Crystals by Tip-Enhanced Raman Spectroscopy. Journal of the American Chemical Society, 2012, 134, 17076-17082.	13.7	42
70	Electrochemistry of robust gold nanoparticle–glassy carbon hybrids generated using a patternable photochemical approach. Journal of Materials Chemistry, 2012, 22, 23971.	6.7	9
71	Mechanism of inhibition of calcium oxalate crystal growth by an osteopontin phosphopeptide. Soft Matter, 2012, 8, 1226-1233.	2.7	31
72	Raman Imaging of Micro- and Nano-Structured Materials. Springer Series in Optical Sciences, 2012, , 119-143.	0.7	0

#	Article	IF	CITATIONS
73	SERS Detection of Streptavidin/Biotin Monolayer Assemblies. Langmuir, 2011, 27, 1494-1498.	3.5	65
74	Covalently Assembled Gold Nanoparticle-Carbon Nanotube Hybrids via a Photoinitiated Carbene Addition Reaction. Chemistry of Materials, 2011, 23, 1519-1525.	6.7	71
75	Mapping Hot-Spots in Hexagonal Arrays of Metallic Nanotriangles with Azobenzene Polymer Thin Films. Journal of Physical Chemistry C, 2011, 115, 15318-15323.	3.1	43
76	Surface patterning using plasma-deposited fluorocarbon thin films for single-cell positioning and neural circuit arrangement. Biomaterials, 2011, 32, 1351-1360.	11.4	29
77	Positionally controlled growth of cells using a cytophobic fluorinated polymer. Analytical and Bioanalytical Chemistry, 2010, 396, 1159-1165.	3.7	9
78	Surface modification of poly(dimethylsiloxane) for microfluidic assay applications. Applied Surface Science, 2010, 256, 2524-2531.	6.1	48
79	Plasmonic properties of Fischer's patterns: polarization effects. Physical Chemistry Chemical Physics, 2010, 12, 6810.	2.8	29
80	Hexagonal Array of Gold Nanotriangles: Modeling the Electric Field Distribution. Journal of Physical Chemistry C, 2010, 114, 19952-19957.	3.1	14
81	Surface-Enhanced Raman and Fluorescence Spectroscopy of Dye Molecules Deposited on Nanostructured Gold Surfaces. Journal of Physical Chemistry C, 2010, 114, 12878-12884.	3.1	44
82	Imaging of single GaN nanowires by tipâ€enhanced Raman spectroscopy. Journal of Raman Spectroscopy, 2009, 40, 1441-1445.	2.5	48
83	Multitip-Localized Enhanced Raman Scattering from a Nanostructured Optical Fiber Array. Journal of Physical Chemistry C, 2009, 113, 874-881.	3.1	38
84	Remote surface enhanced Raman spectroscopy imaging via a nanostructured optical fiber bundle. Optics Express, 2009, 17, 24030.	3.4	23
85	Ultrasharp Opticalâ€Fiber Nanoprobe Array for Raman Localâ€Enhancement Imaging. Small, 2008, 4, 96-99.	10.0	58
86	Preparation and characterization of germanium oxysulfide glassy films for optics. Materials Research Bulletin, 2008, 43, 1179-1187.	5.2	17
87	Raman Enhancement of Azobenzene Monolayers on Substrates Prepared by Langmuirâ^'Blodgett Deposition and Electron-Beam Lithography Techniques. Langmuir, 2008, 24, 11313-11321.	3.5	71
88	Pushing the limit of confocal polarized Raman microscopy. Canadian Journal of Chemistry, 2007, 85, 806-815.	1.1	2
89	Polarized measurements in Raman microscopy. Annual Reports on the Progress of Chemistry Section C, 2007, 103, 326-350.	4.4	12
90	Significant Enhancement of the Optical Second Harmonic Generation in a Poled Azopolymer Thin Grating. Journal of Physical Chemistry B, 2006, 110, 13689-13693.	2.6	10

#	Article	IF	CITATIONS
91	Sensing Vase-to-Kite Switching of Cavitands by Sum-Frequency Vibrational Spectroscopy. Journal of the American Chemical Society, 2006, 128, 12610-12611.	13.7	23
92	Orientation Distribution Functions Based upon Both ã€^P1〉, ã€^P3〉 Order Parameters and upon the Four to ã€^P4〉 Values: Application to an Electrically Poled Nonlinear Optical Azopolymer Film. Applied Spectroscopy, 2005, 59, 322-328.	ñã€^P1ã€% 2.2	‰ up 11
93	Vibrational Circular Dichroism in General Anisotropic Thin Solid Films: Measurement and Theoretical Approach. Applied Spectroscopy, 2005, 59, 732-745.	2.2	104
94	Proton Driven Vase-to-Kite Conformational Change in Cavitands at an Airâ^'Water Interface Monitored by Surface SHG. Langmuir, 2005, 21, 7066-7070.	3.5	9
95	Polarized Raman Confocal Microscopy of Single Gallium Nitride Nanowires. Journal of the American Chemical Society, 2005, 127, 17146-17147.	13.7	70
96	Chromophore Orientations upon Irradiation in Gratings Inscribed on Azo-Dye Polymer Films: A Combined AFM and Confocal Raman Microscopic Study. Journal of Physical Chemistry B, 2004, 108, 6949-6960.	2.6	46
97	Chromophore Orientations in Surface Relief Gratings with Second-Order Nonlinearity as Studied by Confocal Polarized Raman Microspectrometry. Journal of Physical Chemistry B, 2004, 108, 1267-1278.	2.6	37
98	Biaxial Orientation Induced in a Photoaddressable Azopolymer Thin Film As Evidenced by Polarized UVâ^'Visible, Infrared, and Raman Spectra. Macromolecules, 2004, 37, 2880-2889.	4.8	37
99	Chromophore Orientations in a Nonlinear Optical Azopolymer Diffraction Grating: Even and Odd Order Parameters from Far-Field Raman and Near-Field Second Harmonic Generation Microscopies. Journal of Physical Chemistry B, 2004, 108, 17059-17068.	2.6	32
100	Investigation of thermochromism in a series of side-chain, liquid-crystalline, azobenzene-containing polymers. Canadian Journal of Chemistry, 2004, 82, 1-10.	1.1	31
101	Orientation of cavitands at air/water and air/solid interfaces studied by second harmonic generation. Chemical Physics Letters, 2003, 381, 322-328.	2.6	9
102	Synthesis and Characterization of a Series of Azobenzene-Containing Side-Chain Liquid Crystalline Polymers. Macromolecules, 2003, 36, 2680-2688.	4.8	88
103	Surface Vibrational Spectroscopy on Shear-Aligned Poly(tetrafluoroethylene) Films. Journal of the American Chemical Society, 2003, 125, 14218-14219.	13.7	22
104	Poled polymer thin-film gratings studied with far-field optical diffraction and second-harmonic near-field microscopy. Optics Letters, 2003, 28, 1296.	3.3	31
105	Poled polymer thin film gratings studied by near-field second harmonic optical microscopy and far-field optical diffraction. , 2003, , .		1
106	Main Chain-Containing Azo-Tetraphenyldiaminobiphenyl Photorefractive Polymers. Chemistry of Materials, 2002, 14, 168-174.	6.7	51
107	Optical erasures and unusual surface reliefs of holographic gratings inscribed on thin films of an azobenzene functionalized polymer. Physical Chemistry Chemical Physics, 2002, 4, 4020-4029.	2.8	40
108	Photoinduced linear and/or circular birefringences from light propagation through amorphous or smectic azopolymer films. Applied Physics B: Lasers and Optics, 2002, 75, 541-548.	2.2	28

#	Article	IF	CITATIONS
109	Inscription of holographic gratings using circularly polarized light: influence of the optical set-up on the birefringence and surface relief grating properties. Applied Physics B: Lasers and Optics, 2002, 74, 129-137.	2.2	42
110	Time dependent analysis of the formation of a half-period surface relief grating on amorphous azopolymer films. Journal of Applied Physics, 2001, 90, 3149-3158.	2.5	39
111	Dynamics of Photoinduced Orientation of Nonpolar Azobenzene Groups in Polymer Films. Characterization of the Cis Isomers by Visible and FTIR Spectroscopies. Macromolecules, 2001, 34, 7514-7521.	4.8	54
112	Microspectrometric study of azobenzene chromophore orientations in a holographic diffraction grating inscribed on a p(HEMA-co-MMA) functionalized copolymer film. Journal of Raman Spectroscopy, 2001, 32, 665-675.	2.5	21
113	Spectroscopic and Optical Characterization of a Series of Azobenzene-Containing Side-Chain Liquid Crystalline Polymers. Macromolecules, 2000, 33, 6815-6823.	4.8	106
114	Orientation Distribution Functions in Uniaxial Systems Centered Perpendicularly to a Constraint Direction. Applied Spectroscopy, 2000, 54, 699-705.	2.2	45
115	Photoinduced orientations of azobenzene chromophores in two distinct holographic diffraction gratings as studied by polarized Raman confocal microspectrometry. Physical Chemistry Chemical Physics, 2000, 2, 5154-5167.	2.8	53
116	Control of Chirality of an Azobenzene Liquid Crystalline Polymer with Circularly Polarized Light. Journal of the American Chemical Society, 2000, 122, 12646-12650.	13.7	214
117	Polarization analysis of diffracted orders from a birefringence grating recorded on azobenzene containing polymer. Applied Physics Letters, 1999, 75, 1377-1379.	3.3	91
118	Highly Stable Optically Induced Birefringence and Holographic Surface Gratings on a New Azocarbazole-Based Polyimide. Macromolecules, 1999, 32, 8572-8579.	4.8	65
119	Azopolymer Holographic Diffraction Gratings:Â Time Dependent Analyses of the Diffraction Efficiency, Birefringence, and Surface Modulation Induced by Two Linearly Polarized Interfering Beams. Journal of Physical Chemistry B, 1999, 103, 6690-6699.	2.6	82
120	A Raman confocal microspectroscopic study on azopolymer holographic diffraction gratings: Photo― and mass transportâ€induced effects on the molecular orientation. Macromolecular Symposia, 1999, 137, 75-82.	0.7	7
121	Molecular Orientations in Azopolymer Holographic Diffraction Gratings as Studied by Raman Confocal Microspectroscopy. Journal of Physical Chemistry B, 1998, 102, 5754-5765.	2.6	58
122	Photoinduced Orientation of Azobenzene Chromophores in Amorphous Polymers As Studied by Real-Time Visible and FTIR Spectroscopies. Macromolecules, 1998, 31, 7312-7320.	4.8	77
123	Analyses of the Diffraction Efficiencies, Birefringence, and Surface Relief Gratings on Azobenzene-Containing Polymer Films. Journal of Physical Chemistry B, 1998, 102, 2654-2662.	2.6	132
124	Raman Study of the Photoisomerization and Angular Reorientation of Azobenzene Molecules in a DR1-Doped Polymer Matrix. Journal of Raman Spectroscopy, 1996, 27, 491-498.	2.5	35
125	Tip-Enhanced Raman Spectroscopy and Tip-Enhanced Photoluminescence of MoS <sub>2</sub> Flakes Decorated with Gold Nanoparticles. Journal of Physical Chemistry C, 0, , .	3.1	7